Enabling Technologies for Fiber Optic Sensing

Selwan K. Ibrahim*[a], Martin Farnan[a], Devrez M. Karabacak[ab], Johannes M. Singer[ab]
[a]FAZ Technology Ltd., 9C Beckett Way, West Business Park, Dublin 12, Ireland;
[b]Fugro Technology BV, Veurse Achterweg 10, 2264 SG Leidschendam, The Netherlands

Keywords: Fiber optics, fiber Bragg gratings, fiber sensor, sensor interrogation, birefringence, polarization dependent frequency shift, Photonic integration, seismic sensors

Abstract

In order for fiber optic sensors to compete with electrical sensors, several critical parameters need to be addressed such as performance, cost, size, reliability, etc. Relying on technologies developed in different industrial sectors helps to achieve this goal in a more efficient and cost effective way. FAZ Technology has developed a tunable laser based optical interrogator based on technologies developed in the telecommunication sector and optical transducer/sensors based on components sourced from the automotive market. Combining Fiber Bragg Grating (FBG) sensing technology with the above, high speed, high precision, reliable quasi distributed optical sensing systems for temperature, pressure, acoustics, acceleration, etc. has been developed. Careful design needs to be considered to filter out any sources of measurement drifts/errors due to different effects e.g. polarization and birefringence, coating imperfections, sensor packaging etc. Also to achieve high speed and high performance optical sensing systems, combining and synchronizing multiple optical interrogators similar to what has been used with computer/processors to deliver super computing power is an attractive solution. This path can be achieved by using photonic integrated circuit (PIC) technology which opens the doors to scaling up and delivering powerful optical sensing systems in an efficient and cost effective way.

1. INTRODUCTION

In the past couple of decades there has been a rapid development observed in several technological sectors. Such sectors include the semiconductor/processor industry and telecommunications industry. High levels of integration in addition to reductions in cost and power consumption has led to the availability of standard personal computers, laptops and hand held devices (tablets/smart phones) relying on multi-core processers that can deliver performance superior than the super computers developed in the late 1980s and early 1990s (e.g. IBM Cray Y-MP). This has been achieved by utilizing parallel computing techniques via arrays of PCs and microprocessors in addition to reducing the cost and size of microprocessors making high performance affordable machines. The same logic applies in the telecommunication industry and in particular the fiber optic communications sector where wavelength division multiplexing (WDM) is used to increase the number of channels across multiple transmission windows on a single fiber. From the fiber optics communication industry, several optical components have been realized such as tunable lasers that were developed to generate optical carrier signals covering several WDM channels, different optical filtering technologies based on arrayed waveguide grating (AWG) using photonic integrated circuits (PIC) and Bragg gratings technologies. Polarization control/scrambling devices have also been developed to mitigate for different polarization effects in the fibers and optical components. Also real-time high speed processing hardware based on field programmable gate arrays (FPGA) and high speed analog to digital converters (ADCs) have been extensively used for developing high speed fiber optic communication systems and in Radar/Sonar applications.

On the other hand fiber optic sensing has benefited from all the above developed technologies and has been used in various applications (e.g. Energy, Structure Health monitoring, Oil & Gas, Space, Aerospace, Marine, etc.) [1-12]. Here we present a tunable laser based optical fiber sensing interrogator that uses fiber Bragg gratings (FBG) as a sensing element for strain and temperature and is enabled by relying on most of the technology advancements in fiber optic communications to interrogate simultaneously and at high speed multiple FBG sensors all multiplexed in the wavelength domain (WDM) on a single fiber. The optical interrogator relies on a tunable laser (e.g. SG-DBR or MG-Y), which was originally developed for telecom in addition to other standard telecom optical components (e.g. couplers, circulators, Etalons, photo-diodes, etc.), some which can be integrated into a single optical PIC. It also needs low noise electronics and uses high speed ADCs and FPGAs and low cost computer on board (COB) microprocessors (similar to those used in consumer devices) to enable high speed high precision performance.

In addition to the hardware, easy to use software is required to enable the end users who are familiar to electronic sensing systems to use an optical system with high standard and high reliability performance. To achieve the latter, standards and

Optical Sensing and Detection IV, edited by Francis Berghmans, Anna G. Mignani, Proc. of SPIE
Vol. 9899, 98990Z · © 2016 SPIE · CCC code: 0277-786X/16/$18 · doi: 10.1117/12.2234975

test procedures are expected similar to those available in the electronic world. Some effort exists in standardization (e.g. IEEE, SEAFOM, IEC, VDE) [13-20] to define specifications and performance parameters of optical sensing systems, however a lot of effort is still required in order to compare with existing electronic systems. Also in order to measure beyond the fundamental strain and temperature parameters of a standard FBG (typical temperature sensitivity (~10pm/°C), strain sensitivity (~1.2 pm/με)), packaging of the FBG sensor and careful transducer design in combination to low noise high precision interrogation techniques are required to enable other measurements such as pressure, acoustics, acceleration, etc. for static (DC) and dynamic (AC) applications that could be used in different industries and environments. Figure 1 below shows a pyramid chart representing the main elements that defines a fiber optic sensing system starting from the basic sensing element (e.g. FBG) that inherently can measure strain and temperature. To measure beyond that, a transducer sensor has to be designed to translate other physical effects (e.g. Pressure, acceleration, acoustics, etc. to strain on a FBG. The sensor needs to be connected to a measuring device via an optical fiber designed to survive different environments. The measuring device is called an optical interrogator that detects the optical signal response and converts it to a measurement generating data which is then displayed or logged/stored for further processing and analytics. Each section of the pyramid relies on technologies developed for different industries and applications (e.g. fiber optics telecommunication, computer and parallel processing, Radar/Sonar, DSP, 3D printing, web technology, data analytics, etc.) as shown in figure 1. Also when comparing the pyramid diagram to an electronic sensing system, the sensing element could be a resistive element which is used to build a strain gauge or a thermistor connected via twisted copper wires to a bridge circuit and a low cost portable multi-meter. All which is based on low cost, easy to use, and widely available technology. Today optical sensing technology can deliver the desired performance in several specific industries. However, for it to be widely used and considered as an alternative to current electronic sensing systems in a wider range of applications, it needs to be competitive in price, easy to use, while maintaining the desired performance which can be achieved by relying on current technologies to reach this goal.

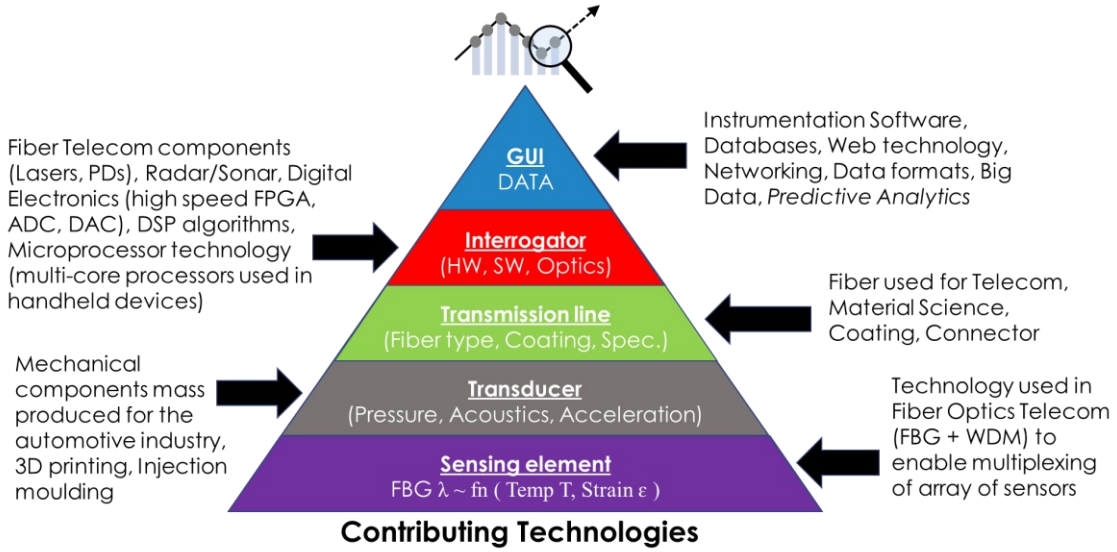

Figure 1. Fiber optic sensing system and contributing technologies.

2. FBG OPTICAL INTERROGATOR

The operation of a typical tunable optical interrogator is shown if figure 2 below consisting of a source based on a tunable laser. In other types of optical interrogators the source could be a broadband/comb based source or an array of lasers. The output of the source is split into different fibers (for a multi-channel system) and connected to an array of couplers or circulators that interface between the fiber containing the sensors and the receiver which detects the reflected response from the FBGs and converts it to an electrical signal which is then sampled using analog to digital converters (ADC) for further processing in the digital domain. The data is then formatted and transferred over a data bus (e.g. Ethernet, Serial, USB, etc.) to a client for feedback control/storage/analysis. In other types of interrogators where a

broadband source is used in a wavelength multiplexing system, a filter/AWG would be typically used to separate the different wavelengths. It is also possible to use time division multiplexing (TDM) in combination with WDM by multiplexing multiple spatially spaced FBGs located within a certain wavelength band in the time domain by making the FBGs having low reflectivity and similar wavelengths. The reflected signals are then detected/demodulated using different techniques (phase detection (coherent/interferometric), OFDR, pulsing, etc.). However the interrogator hardware and processing gets more complex and expensive and is not covered in this paper.

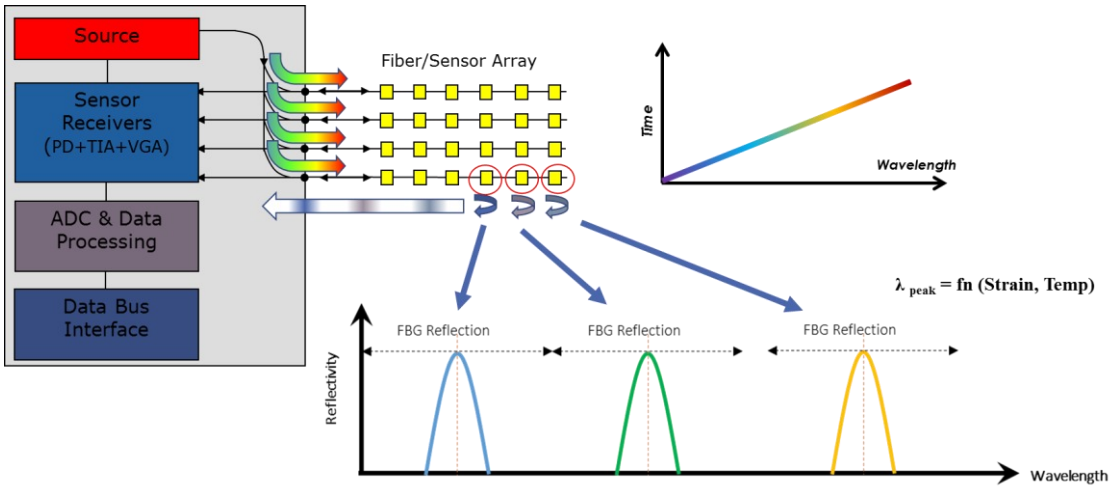

Figure 2. Operation of a typical FBG tunable laser based optical interrogator

In order to define the performance of a measurement system, one needs to determine the reproducibility of the measurements as well as any repeated (systematic) errors the system can contain. For these, the following terms are commonly used in the field as shown in figure 3;

- Precision: Represents the minimum resolvable change in wavelength It is also defined as the deviation of a set of measurements over a specified timeframe, reported here as peak-to-peak or 1σ standard deviation. The latter approach is a commonly employed practice in the industry for datasheets and is most appropriate when using large datasets and long timescales (i.e. statistically significant number of points). When using small datasets and short time scales, peak to peak measurements are considered to be more applicable.
- Accuracy or Systematic Bias (Trueness): The deviation of the precision measurement to a true reference value. In the case of an optical interrogator, the reference value is the wavelength of an absorption gas line trough defined by the NIST HCN standard [21]. Once measured, this bias can be used as a correction offset when the interrogator is used as part of a larger system (i.e. calibrated). In this paper the term Accuracy is used.

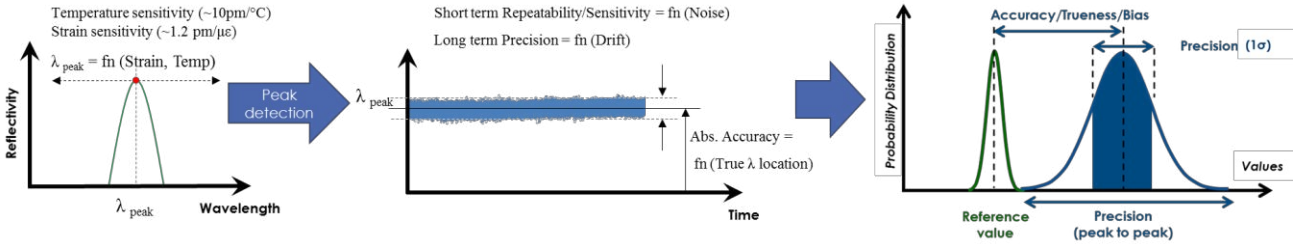

Figure 3. Description of accuracy and precision for FBG optical interrogators

Currently there is no common standard adapted by all optical interrogator and FBG sensor manufacturers. However there has been several recent activities carried out by several standardization groups to cover different aspects of optical fiber sensor standards e.g. IEC 61757-1:2012, VDI/VDE 2660 [17, 18]. There has also been application specific workgroups developing standards and guidelines such as SEAFOM [19] which is an international joint industry forum with the goal to promote the growth of fiber optics in subsea and all upstream oil and gas industry applications. IEEE has also recently started activities in fiber optic standards IEEE (IC15-001-01) [20] with the aim to cover standards for optical sensing

systems used for different applications. The IEEE Ethernet 802.3 [22] working group offers a wide range of standards extending to Gigabit Ethernet is a good example on how the standard has evolved over the years from Ethernet over twisted pair to optical fiber and is a common standard used by Ethernet equipment manufacturers. An equivalent for the optical sensing industry would be very beneficial and could make the fiber optic industry more competitive.

3. FAZT TUNABLE LASER INTERROGATOR PLATFORM

The FAZ Technology (FAZT) tunable laser based optical interrogator platform (V4 and I4) is based on a semiconductor tunable laser diode that has no moving parts delivering high level of reliability and accuracy in addition to a power and wavelength reference section that includes several fine and coarse periodic wavelength references (e.g. Etalon). The main basic building blocks of the interrogator is shown in figure 4 below consisting of the transmitter section, polarization controller/scrambler, passive optics section which interfaces between the fiber sensor array and the receiver section, all connected and controlled by a computer on board (COB) which transfers the data to the end user/client via a high speed data communication link. The polarization switch/scrambler is connected between the laser output and the FBG channels for polarization control and polarization dependent frequency shift (PDFS) mitigation [23].

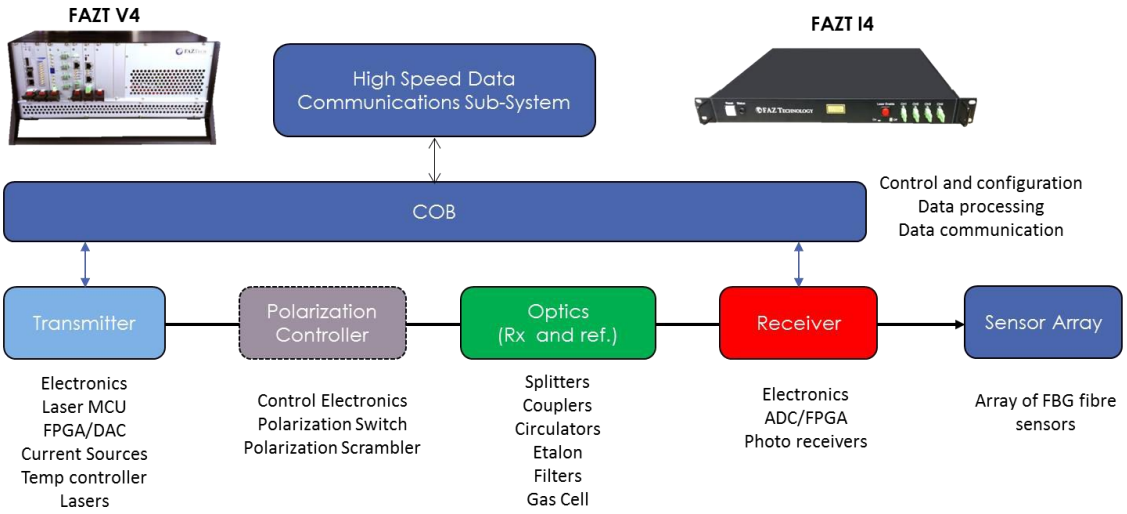

Figure 4. Block diagram of the FAZT tunable laser interrogator

The high resolution specification is achieved by using a highly repeatable calibrated tunable laser designed for stable operation over its life time (>15years) and combined with precise wavelength referencing to correct for any short term noise and long term drifts. The laser in the V4/I4 interrogator scans the C-band (40nm) at a rate of 1kHz (tuning rate of 0.1pm/ns) and the output power is split over four separate channels (typically +3dBm/channel) as shown in figure 5 with the minimum detectable power (noise floor) at the receive end <-40dBm. The received reflected signal is sampled with 1pm resolution. The four separate fiber optic channels can each simultaneously measure up to 30 FBG sensors @ 1 kHz sample rate (120 sensors in total). This is achieved by implementing the FBG peak processing algorithms in hardware on a field programmable gate array (FPGA) connected internally to a computer on board (COB) unit which enables streaming data over a 1Gbit/s Ethernet connection for the V4, and 100Mbit/s Ethernet connection for the I4.

It should also be noted that the key critical components of the system (Tunable Laser and Etalon) were tested and validated for use in a launcher environment as part of an European Space Agency (ESA) GSTP project by subjecting them to extreme temperature and vibration tests [11]. The vibration tests included resonance tests up to 2.5g, sinusoidal tests up to 22.5g, and random vibration tests up to 20g all over 3-axis within a 5-2000Hz frequency range, while the thermal tests covered an operating range from -20°C to +70°C [11]. Different technologies and standards were used in the development of the integrator. The V4 system was based on an Open VPX-VITA 46 backplane standard (typically used in aerospace/defense) and uses commercial off-the-shelf (COTS) components such as a computer on board based on an Intel i7 quad-processer running Windows 7 and the FPGA/ADC board which is designed for different applications (e.g. Radar/Sonar and communications). The V4 was designed for high performance instrumentation mainly targeting the development and prototyping of advanced sensors and different interrogation algorithms offering spectral data

delivery at high speeds (e.g. 40nm@200/1000Hz with 1/5pm resolution) in addition to the ability to easily interface to electronic sensing systems. On the other hand the I4 is designed as a robust and cost effective interrogator for deployment in various industrial applications. It is also based on mass produced cost effective components (e.g. industrial version of a COB based on an OMAP4 Cortex-A9 Processor running Linux) which is used in different portable consumer products (e.g. Amazon Kindle Fire and other tablets).

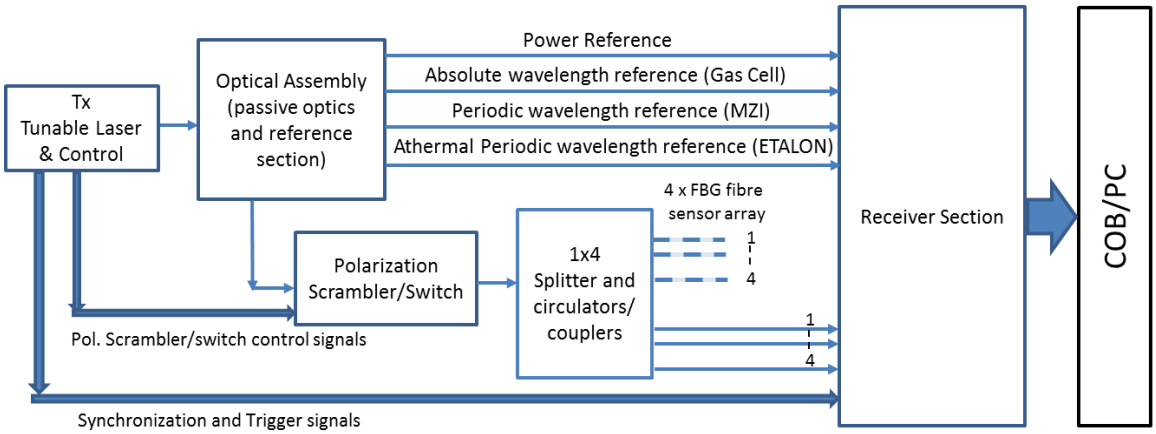

Figure 5. Schematic diagram of the FAZT tunable laser interrogator

4. INTERROGATOR PERFORMANCE

To demonstrate the long term absolute (DC) performance of the interrogator system, a benchmarking test was performed by connecting a 10 Torr HCN gas cell to one of the four optical channels of the FAZ V4 interrogator as shown in figure 6 (top-left). In this test, three of the gas lines as shown in the table in figure 6 (bottom-left) have been selected. The troughs of the gas cell were processed and the distribution of the samples showing the spread over time is observed in figure 6 (bottom-right) and compared with another commercial swept laser interrogator.

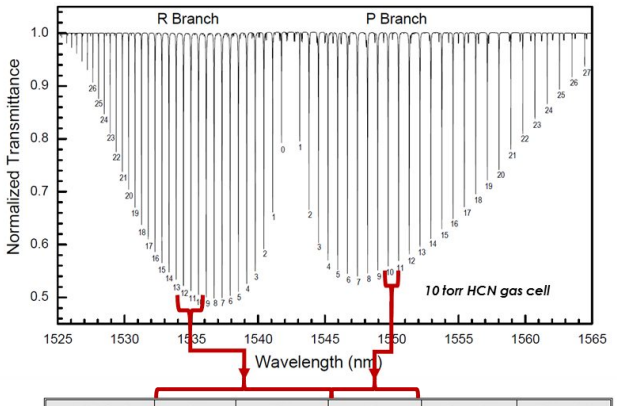

HCN GAS CELL LINE	R12 1534.41503	R11 1534.97249	P10 1549.73058	R12 – R11 (-0.557460)	R11 – P10 (-14.75809)
Precision (pk-pk)	86 fm	124 fm	166 fm	168 fm	191 fm
Precision (1σ)	15 fm	25 fm	30 fm	34 fm	30 fm

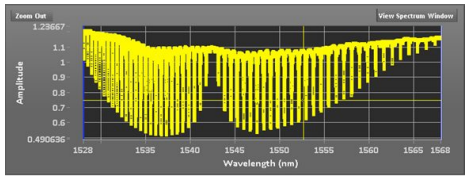

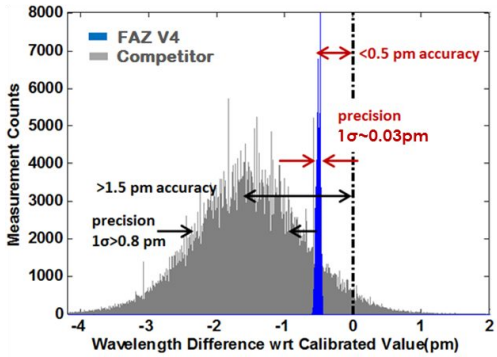

Figure 6. NIST Specified spectrum of a HCN Gas Cell, with the 3 lines used here are marked (top-left), Precision and Accuracy to reference of P10, R12, R11 HCN Gas lines calculated for the entire dataset (bottom-left), Spectrum of HCN gas cell captured using the V4 (top-right), Histogram of ~61 hours measurements for the P10 gas line (10 Torr) for FAZT V4 (averaged down to 2Hz) vs competitor data (2 Hz) (bottom-right).

The absolute test was repeated on the I4 as shown in the histogram in figure 7 (left) below showing the spread of the P10 gas cell tracking over 10 hours vs. a competitor tracking of the same gas cell using a swept source interrogator. The

deviation of 42 HCN gas cell lines from there specified value [21] tracked across the full C-band at room temperature over several scans is shown in figure 7 (bottom-right) where the max peak-to-peak spread is <0.7pm and max deviation from the HCN gas cell reference data sheet was <0.33pm.

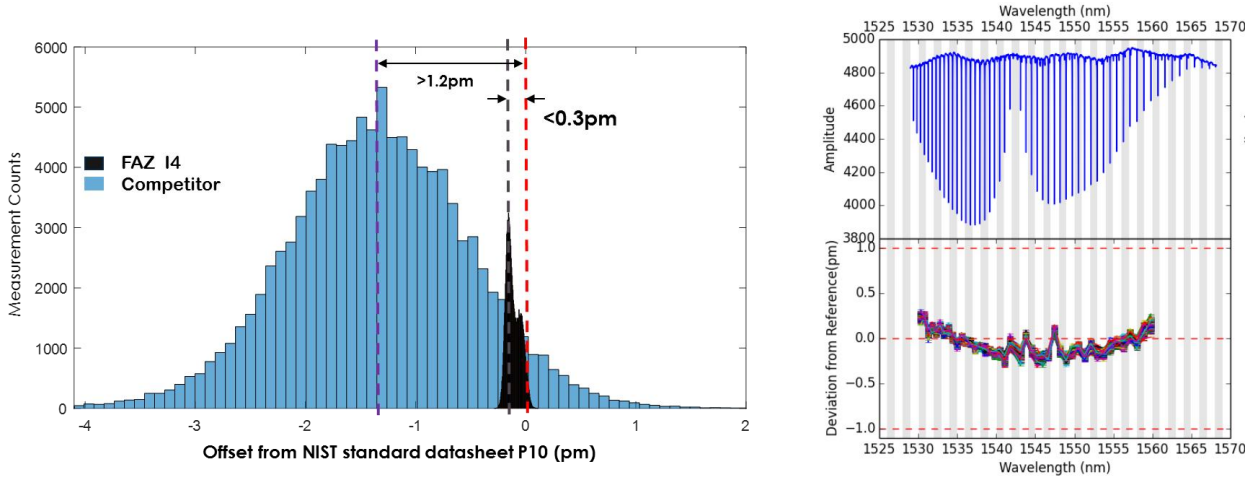

Figure 7. Histogram of >10 hours measurements for the P10 gas line [1549.7305] for FAZT I4 (down sampled to 2Hz) vs. competitor data (2 Hz) (top-left),Spectrum of HCN gas cell captured using the I4 (top-right), Deviation of measured troughs vs. HCN specification across the C-band (bottom-right)

From figures 6 and 7 it was demonstrated that the highly repeatable tunable laser combined with precise wavelength referencing enables long term high precision measurements (DC) (precision <30/100fm (1σ) (V4/I4) measured by tracking HCN Gas Cell line P10 [1549.7305] [21]). The V4/I4 long term absolute accuracy specified over the life time of the product (bias/deviation from the true value using a HCN gas cell) over the operating target temperature (0-55°C) and wavelength range (C-band) is <1pm. This may be improved to <0.5pm when operating at room temperature for both V4/I4. For dynamic measurements (AC), a repeatability of <25/50fm (1σ) @1kHz sample rate is achieved for the V4/I4. Also due to the high resolution sampling (1pm), narrow FBGs can be interrogated as shown in figure 8 where the peak of a FBG with a 40pm full width half maximum (FWHM) was tracked @1kHz sample rate over 40 seconds. The slow drift was due to the FBG drift with temperature and the p-p noise was measured to be ~50fm. The repeatability (standard deviation) measurement of the de-trended (AC) un-filtered data (@500Hz BW) was measured to be 12.4fm, while the filtered (@80Hz BW) standard deviation was measured to be 4.3fm (<5fm). This reflects the minimum detected wavelength shift of a FBG peak which represents a low noise floor in the frequency domain. It is also used to define the dynamic range measurement for an acoustic frequency measurement (e.g. vibration tones and acoustic frequency measurements) which is important is seismic applications.

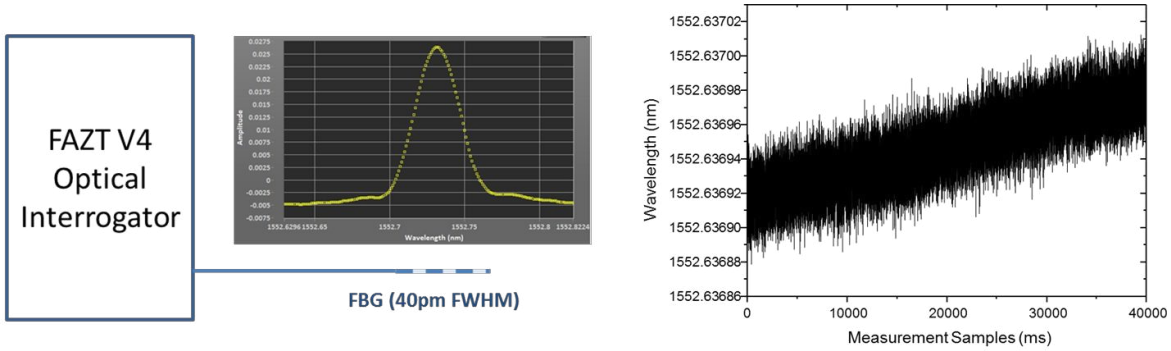

Figure 8. V4 peak tracking@1kHz sample rate for a narrow FBG with 40pm FWHM over 40 seconds

The FAZ interrogator uses a laser with a polarized output and includes the option to interrogate and mitigate polarization effects for different types of sensors using either a 2 state polarization switch, a multi-state (>2) polarization switch, or a high speed scrambler which could be required for certain applications. Polarization dependent frequency shift (PDFS) in

FBG sensors are due to inherent birefringence in the FBG due to the fiber or due to transversal strain applied on the FBG during mounting/packaging of the sensor and could be > 1pm up to 40pm and higher depending on the type of FBG and birefringence induced. Figure 9 (bottom) below shows a simple setup where a FBG was placed in a stable temperature controlled environment (a calibrated dry block) and interrogated with the V4 interrogator while a polarization scrambler was placed in the transmission path of the polarized laser to emulate the change of polarization state in the fiber (due to temperature or movement of the fiber) by generating 200 random polarization states covering the Poincare Sphere. The detected peaks are then averaged with and without the polarization switch turned on and the results are shown in figure 9 (top) where the peak-to-peak FBG tracked peak changed from ~14pm to ~1.4pm giving a factor of 10 reduction in PDFS. The PDFS reduction factor varies and depends on several variables such as the polarization mitigation technique used, type and shape of FBG, birefringence, speed of polarization change, averaging, etc.

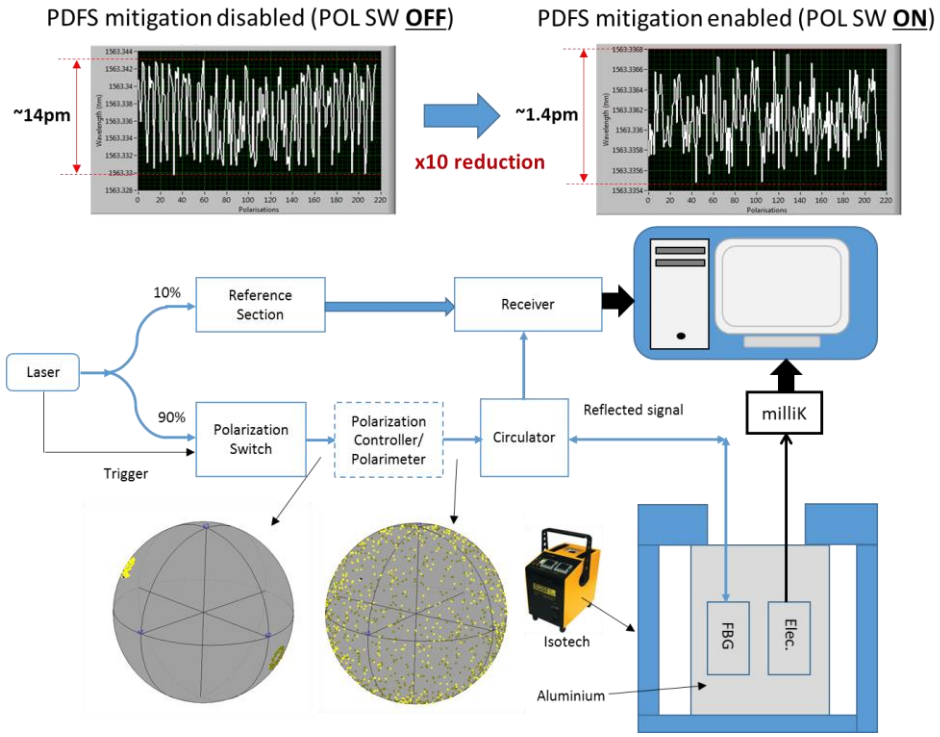

Figure 9. Polarization emulation setup using a programmable polarization controller/scrambler in optical path (bottom), and reduction in PDFS for the tracked stable FBG peak when the polarization mitigation is OFF (top-left) and ON (top-right)

In many applications where a measurement over longer periods of time is required, greater attention needs to be focused on the timescales of the measurement fluctuations in relation to the "observation time scale". The observation time scale can be considered as the time scale within which measured data needs to be correlated. For example, for recording of steady-state vibrations with the signal of interest falling within a frequency bandwidth of f_{bw}, a sampling frequency of fs > $2f_{bw}$ is required (Nyquist sampling theorem) and an observation time scale typically t > $5/f_{bw}$ is needed. Background fluctuations on a longer time scale (like temperature changes) can be filtered out, for example by using high pass filter (HPF) techniques. Similarly, in seismic applications (non-steady state vibrations) for example, the observation window can be set as the time gap between air gun shots (i.e. few seconds) and any fluctuations on a longer time scale can again be filtered out using a high pass filter (HPF). However, if the application requires the recording of a quantity (e.g. pressure) continuously over days (e.g. for a valve control system), one needs an "observation timescale" of days/weeks/months. In such situations, fluctuations in the sensor, connections, and the interrogation system can play a dominant role and cannot be filtered out by high-pass filtering. In order to evaluate the interrogators suitability for these applications an alternative view based on observation timescales for the HCN gas line P10 can be generated as shown in figure 10 where the highest standard deviation (worst case) obtained for a range of observation time scales for each set of averaged data is plotted.

Having established a base line for the precision and accuracy of the interrogator, the focus is shifted to its application for measurements of FBG sensors, for long term and short term measurements. One approach for determining the precision and accuracy of measuring an FBG is to control the environment as precisely as possible, placing the FBG sensors in that environment and then running the same tests as used for the long term Gas Cell measurements. However, maintaining the environment to the level of precision necessary to establish a baseline for an extended test run using FBGs is difficult to achieve especially considering their temperature sensitivity. In the gas cell test where we demonstrated precision of 30fm over 60 hours it would mean having to maintain a temperature controlled environment for the same time period at better than 0.003°C (using a guide of temperature sensitivity of an FBG as 10pm/°C).

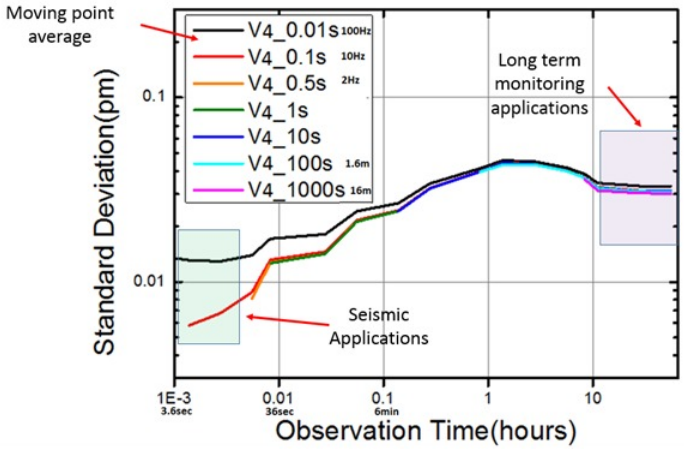

Figure 10. Standard deviation (worst case) measurement of a HCN gas line P10 (1549.7305nm), with different averaging

The alternative approach selected is to place two FBGs from the same supplier in the same environmental conditions. The wavelength difference between the measured values (FBG1 – FBG2) will represent the precision that can be obtained over the timescale of the experiment. Furthermore, it is a clear indication of the level of temperature compensation one can expect to achieve when developing various strain based sensor systems using FBGs. Figure 11 (top-left) shows two example FBGs in separate glass capillary tubes placed closely together and taped to a board. The V4 interrogator was operated to record the FBGs at 1 kHz (full 40nm wavelength range), averaged down to 2 Hz with figure 11 (bottom-left) showing the wavelength change for both FBG sensors over a 24 hour duration.

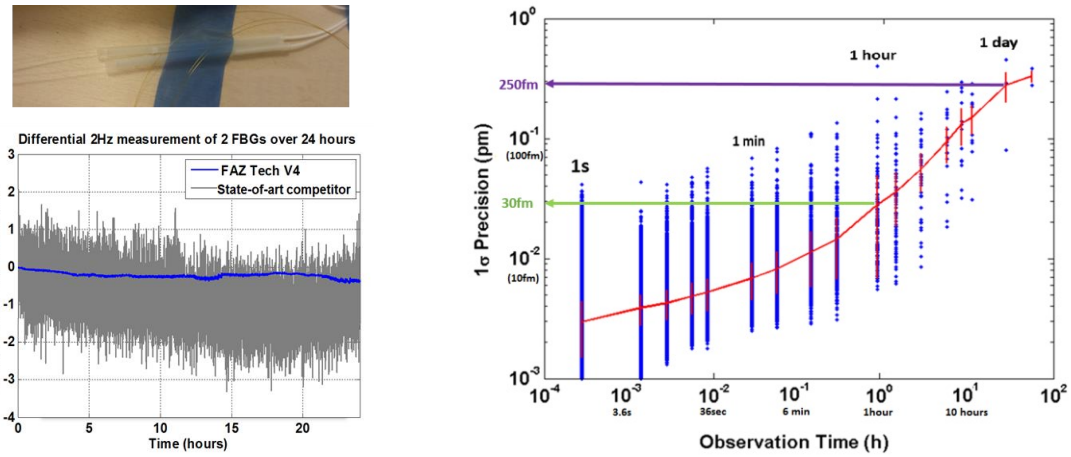

Figure 11. 2 FBGs in glass capillary (top-left), differential measurements using FAZT V4 at 2 Hz (0.5s averaging time) vs. competitor at 2 Hz (bottom-right), precision of the FAZ interrogator in differential tracking of FBGs over a wide range of observation timescales (right).

Figure 11 (right) shows the standard deviation based on the observation time using the 110 hours of 2 Hz dataset. For an observation time of 1 hour, the standard deviation (1σ) is 30fm, this increases to 250fm for a 24 hour observation time and remains below 500fm (0.05 °C) for the entire measurement time. Figure 12 shows that the results are fiber dependent

and are different for different FBGs from different suppliers where the obtained precision results were found to be >3pm for some FBGs and as low as 0.1pm for others, indicating that the interrogator system is not the only limiting factor for a baseline measurement (as shown from the gas cell measurements in figure10) and the combination of interrogator + sensor is critical to define any system performance. Several factors ranging from FBG manufacturing techniques, FBG spectral response shape, birefringence and polarization dependency (e.g. PDFS), coating type and uniformity, pre-straining and packaging of FBGs, etc. are all contributing factors to this drift and could be optimized to improve the overall system performance by working closer with FBG suppliers.

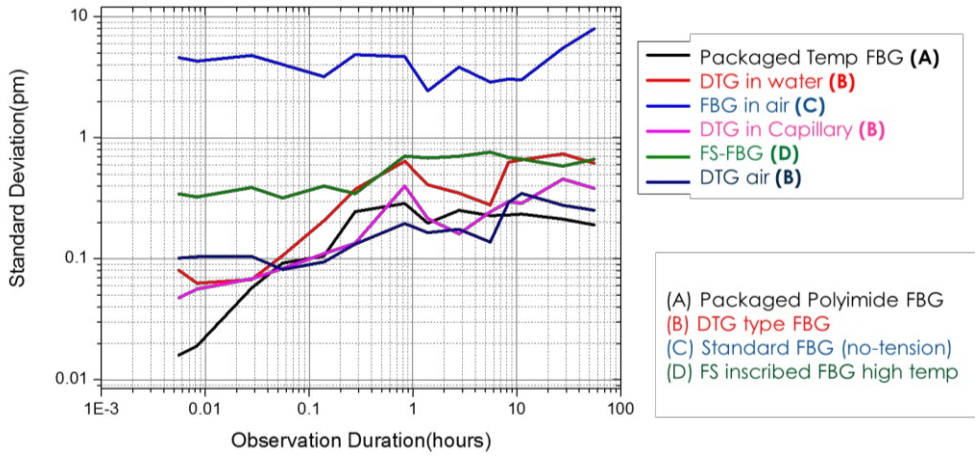

Figure 12. Standard deviation (worst case) obtained in differential tracking of FBGs from 4 different FBG manufacturers.

In many dynamic applications, the observation window is short, corresponding to measurements of transient effects (e.g. seismic reflections that occur after firing of air gun arrays or vibrator sources). The results indicate that a standard deviation of a few fm is achievable in filtered data. Such low noise level results enable the development of optical accelerometers with <µg level resolutions, hydrophones with sub-Pascal sound pressure resolution and sensors that reach >120 dB dynamic range.

5. FBG OPTICAL SENSORS

Optical sensing using standard FBGs offer two fundamental measurements; strain and temperature. Using the V4 (with the polarization SW enabled) to interrogate a DTG based temperature probe tested in a calibrated dry block with a high precision thermometer, an absolute accuracy of ±0.1°C measured over the full temperature cycle -20°C to +80°C as shown in figure 13 below [11].

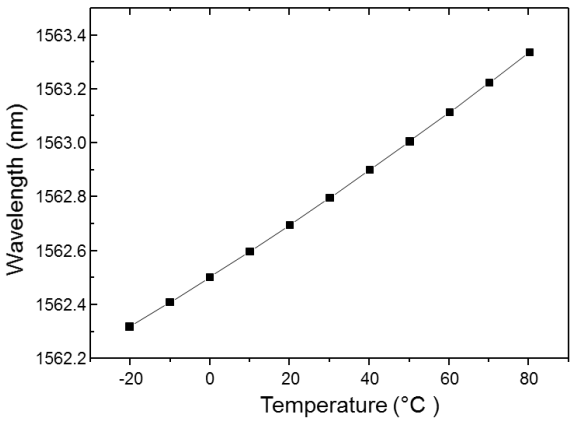

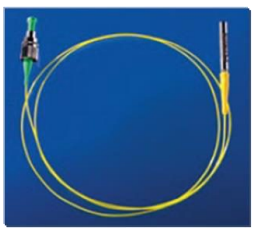

Parameter	Value
Sensor temperature range	-20°C to +110°C
Sensor length	58 mm
Housing diameter	5 mm
Housing material	SS316

Figure 13. Tracked FBG peak wavelength vs. temperature for a DTG based temperature probe.

Another test was carried out to measure the FBG response against a calibrated electrical strain gauge with the objective to demonstrate micro-strain measurements of ±1200µε, using three electrical strain sensors (typically used for space

applications), and two FBG strain sensors mounted on both sides of a calibrated cantilever system as shown in figure 14 (left). Similarly with mitigating the PDFS of the FBG strain sensor, the results showed a difference in accuracy of ±3με for the concave, and ±4με for the convex as shown in figure 2 (right) [11].

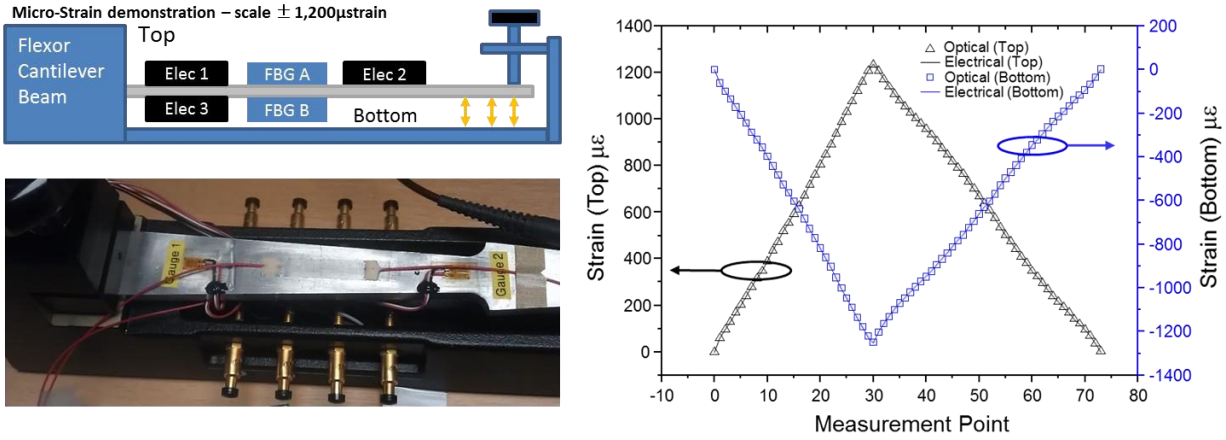

Figure 14. Strain measurements for optical/electrical strain sensors mounted on both sides of a cantilever

FBG optical sensing systems can offer much more than just strain and temperature sensing and offer a wide variety of sensing opportunities due to their large linear range, high speed and accuracy possible in combination with high resolution interrogation. Designing packaged FBG based sensors (transducers) with high sensitivity (>10x higher sensitivity when compared with standard FBG sensitivity 1.2pm/με) and when combined with the low noise level of the FAZT interrogator at relevant frequencies (>×100 better noise floor compared to available commercial swept source interrogators), a combined resolution benefit >×1000 and dynamic ranges >120dB can be achieved making the performance competitive with electrical sensing systems.

The high resolution of the FAZ interrogator and the geoscience know-how of Fugro has led to a development of a portfolio of high resolution FBG-based sensors such as Hydrophones, Accelerometers, Pressure, Sound, Vibration and Tilt sensors suitable for different applications as shown in figure 15 below.

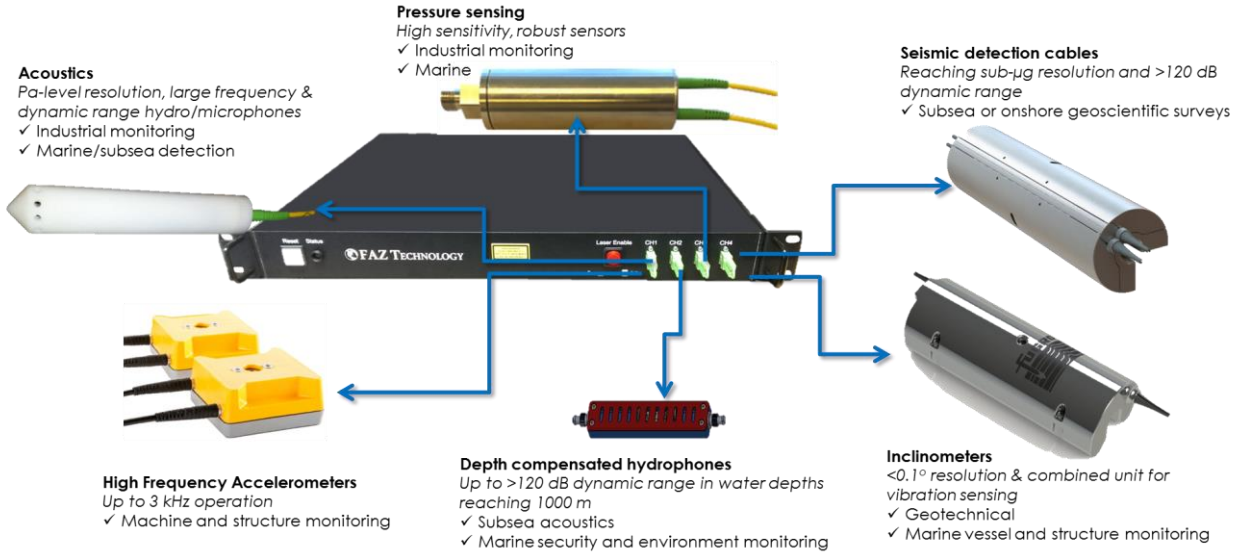

Figure 15. FAZ-Fugro range of FBG based optical sensors.

To design a FBG pressure sensor, a transducer design must be used to translate pressure to linear strain on a FBG. Pressure gauges can be used to measure both static and dynamic (sound) pressure (e.g. hydrophones) for different applications where a wide linear operation range is required. This can be achieved by using a pressure deformable body (commonly used in the automotive industry) to translate pressure changes to linear strain as shown in figure 16.

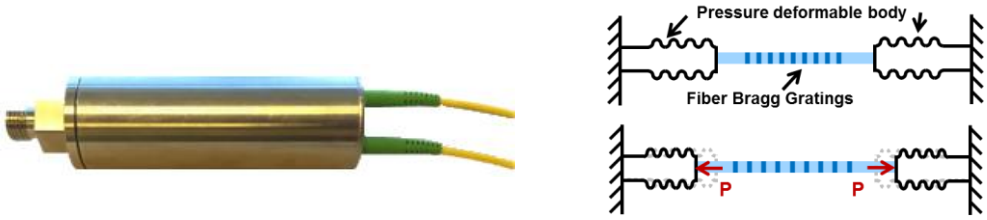

Figure 16. FBG based Pressure sensor

The proposed high-accuracy pressure gauge based on FBG technology allows for passive (electrical power-free) remote monitoring of absolute, differential or relative pressures, for both liquid and gaseous environments. It also supports a 2-fiber port configuration allowing for chain formation with a variety of FBG-based sensors on a single fiber and can be ruggedized for harsh environments. The pressure range can be tuned based on the application and design (e.g. for marine application absolute pressure up to +3 bar and sensitivity >6 pm/mbar). The temperature range depends on the FBG type used and application (typically -20°C to +60°C for marine) and the resolution is typically <0.1% full scale while the accuracy is <1% full scale.

On the other hand acceleration can also be turned into fiber strain where the main challenge is to find the optimum trade-off in sensitivity vs. resonance frequency vs. size, where the sensitivity ~ force on fiber, force on fiber ~ inertial mass, and resonance frequency ~ √(stiffness/mass). Very different range of accelerometers are possible with one architecture delivering µg and sub-µg level resolution, high dynamic range and low noise performance when combined with the FAZT interrogator. Figure 17 (left) shows different accelerometer designs and a comparison between an optical FBG accelerometer vs. an electrical reference accelerometer in the time domain both exposed to the same excitation signal (Figure 17 (top-left)). Figure 17 (right) shows the frequency response of different FBG accelerometers designed for different applications where different resonance frequency vs. sensitivity tradeoffs have been tuned. These accelerometers can be used for both dynamic (AC) and static (DC) applications (e.g. seismic, geotechnical analysis, machine and structure monitoring). The frequency range could be tuned between DC and 200/1000/3000Hz delivering sensitivities >1000/80/4 pm/g and operation range of ± 2/40/500 g with an accuracy of 1% full scale, phase flatness <±5 degrees, linearity <±1dB sensitivity flatness, and cross-axis interference <-30dB.

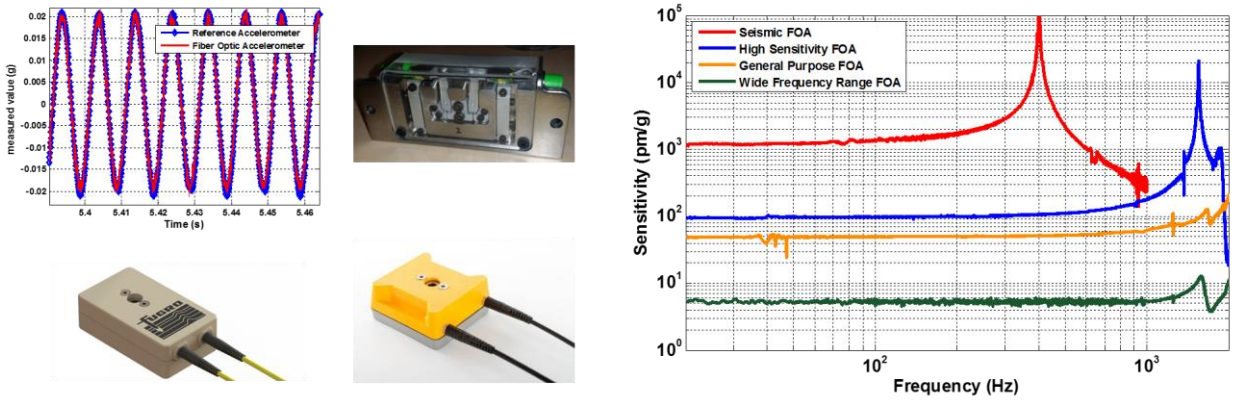

Figure 17. FBG based accelerometer sensor (left), and frequency response (right)

Typically for static measurements (Strain. Pressure, etc.), a second FBG would be required located in or close to the package to compensate for the temperature drifts in the main measurement FBG. However as discussed in the previous section as shown in figure 12, differential tracking of FBGs from different suppliers have shown a baseline limit for accuracy measurements due to the different characteristics of different FBGs and the difficulty to make sure both FBGs

are exposed to the exact same temperature which is required for very accurate measurements. On the other hand it is possible to interrogate other types of FBG sensors (e.g. Birefringent FBGs) [24-27] with the interrogator polarization control feature. Such FBGs can be used to simultaneously measure Strain and Temperature (polarization maintaining FBG (PM-FBG)) [25, 26] as shown in figure 18 where the temperature variation and stability during a strain calibration measurement was found to be approximately ±0.2°C, or/and measure temperature independent pressure using micro-structured fiber FBG (MS-FBG) [27].

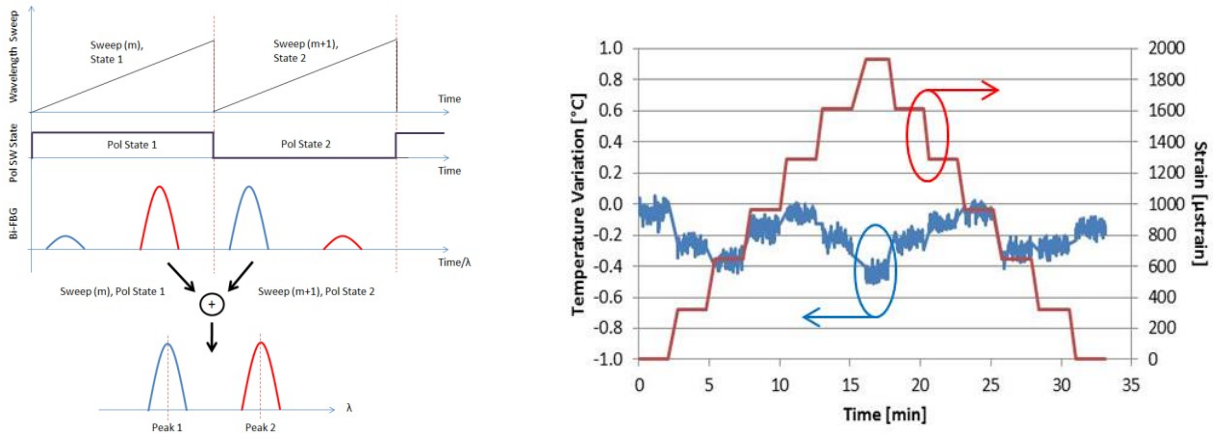

Figure 18. Interrogation technique for Bi-FBG using spectral averaging (left), calculated temperature variation during the strain calibration together with the applied strain profile (right)

Also for high temperature applications >700 °C, other type of sensors that can be interrogated using the same tunable laser interrogator platform become more attractive (e.g. Femtosecond inscribed FBGs, Sapphire FBGs, Fabry Perot (FP), Multi-Core fiber sensors (MCF), etc.) [28-30].

6. HOW TO INCREASE THE PERFORMANCE FURTHER?

In the previous section it was demonstrated that by combining a high speed, high resolution tunable laser interrogator with a high sensitivity FBG sensor with an optimized transducer design, it is possible to reach dynamic ranges >120dB and start competing with electrical systems. To improve the performance and at the same time scale up the number of sensors, further improvements would be required. This can be achieved by applying the same techniques deployed in the computer industry by running multiple computers and processors in parallel to achieve a super computer performance at a low cost. The same logic can be applied to interrogators where it is possible to extend the wavelength range of a tunable laser to support more sensor bands in the wavelength domain and sweep over different wavelength bands at higher speed (e.g. 1kHz@40nm to 4kHz@10nm with tuning rate 0.1pm/ns) as shown in figure 19 or higher tuning rate (8kHz@10nm with tuning rate of 0.2pm/ns).

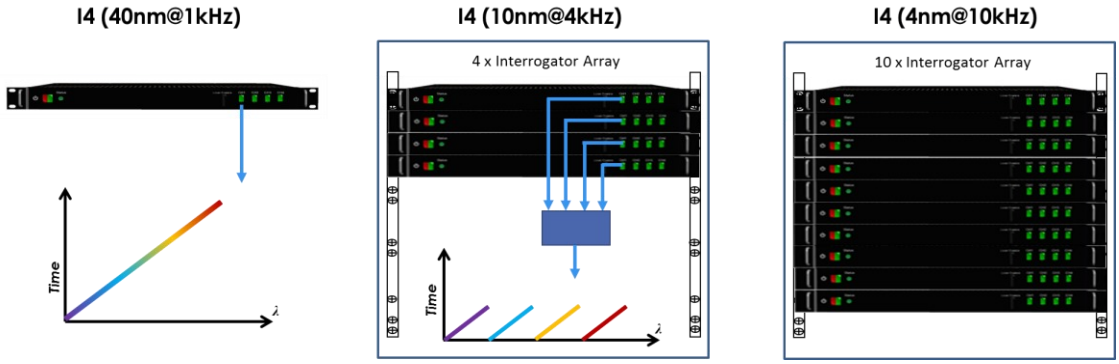

Figure 19. Networking multiple interrogators to sweep at high speed over different wavelength bands (parallel interrogation)

The higher speed enables oversampling and would result in better noise floor which would improve the overall sensor dynamic range assuming Gaussian noise characteristics. It also enables the implementation of a digital anti-aliasing filter which is typically implemented in the electronic world by using a low pass filter (LPF) in front of the ADC.

To reduce the footprint and cost of combining a large number of interrogators networked together, photonic integration would be needed. Micro-processors have benefited from electronic integration and Moore's law where we can see very powerful multi-core processers commercially available and used in today consumer products. A photonic integrated circuit (PIC) is a solution to achieve low-cost, small footprint reliable optical sensing systems that could compete with electronic systems in performance, cost and size [31-33]. There exists several technology platforms (e.g. InP, Si, TriPlex) that could be used to develop different optical building blocks used in the interrogator shown in figure 4 and 5. Such building blocks include the tunable laser, couplers, photodiodes, polarization switch, MZIs, SOAs, delay lines, etc. where most are available on the InP platform. The next generation photonic integration platform would include hybrid integration where the best of each platform could be used to build different devices and combined together and connected to the electronic world using CMOS technology which is mature in the electronic chip industry [31].

An example of the photonic integration of the interrogator is demonstrated in the design of the reference and receiver section of the interrogator which replaces 80% of current discrete optical components (splitters, combiners, MZI, photodiodes) and reduces the number of splices in the system. The design and chip manufacturing was carried out as part of an InP multi-project wafer (MPW) run under the EU PARADAIGM project [32, 33] as shown in figure 20. The next generation interrogator PIC is planned to include a tunable laser. More work needs to be done to make the technology mature further and offer low cost commercial packaging options to reduce the overall cost in order to compete with low cost electronic sensing systems.

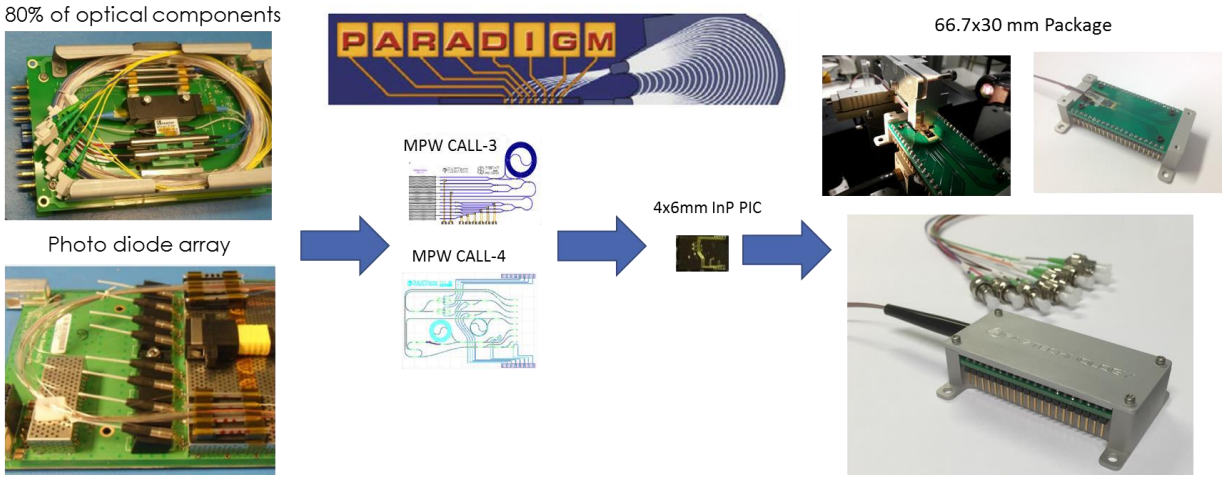

Figure 20. Photonic integration using InP MPW to replace 80% of discrete optical components in the interrogator

ACKNOWLEDGMENTS

The authors would like to thank all the FAZ Technology engineering team and Fugro sensor development team. This work was supported by the ESA programs GSTP, FLPP, ARTES and the EU PARADAIGM project.

REFERENCES

[1] Kersey, A.D., Davis, M.A., Patrick, H.J., LeBlanc, M., Koo, K.P., Askins, C.G., Putnam, M.A. and Friebele, E.J., "Fiber grating sensors," IEEE Journal of Lightwave Technology, 15(8), 1442-1463, (1997).

[2] Thévenaz, L, "Next generation of optical fibre sensors: new concepts and perspectives" 23rd International Conference on Optical Fiber Sensors (OFS2014), Proc SPIE 9157AN, (2014).

[3] Lindner, E., Mörbitz, J., Chojetzki, C., Becker, M., Brückner, S., Schuster, K., Rothhardt, M., Willsch, R. and Bartelt, H., "Tailored draw tower fiber Bragg gratings for various sensing applications," Asia Pacific Optical Sensors Conference, 835112-835112, (2012).

[4] Willsch, R., Ecke, W., Rothhardt, M.W. and Bartelt, H., "Advanced Optical FBG Sensor Systems and Examples of Their Application in Energy Facility Monitoring," Advanced Photonics Congress Bragg Gratings, Photosensitivity, and Poling in Glass Waveguides, BTu4E-1, (2012).

[5] Alwis, L., T. Sun, and Grattan, K.T.V., "Developments in optical fibre sensors for industrial applications," Optics & Laser Technology, 78, 62-66, (2015).

[6] Kinet, D., Mégret, P., Goossen, K.W., Qiu, L., Heider, D. and Caucheteur, C., "Fiber Bragg grating sensors toward structural health monitoring in composite materials: Challenges and solutions," Sensors, 14(4), 7394-7419, (2014).

[7] Mihailov, Stephen J., "Fiber Bragg grating sensors for harsh environments," Sensors, 12 (2), 1898-1918, 2012.

[8] Baldwin, Christopher, "Optical fiber sensing in the oil and gas industry: overcoming challenges," OFS2014 23rd International Conference on Optical Fiber Sensors, Proc. SPIE 9157C4, (2014).

[9] Skinner, N.G. and Maida, J.L., "Downhole fiber optic sensing: the oilfield service provider's perspective: from the cradle to the grave," SPIE Sensing Technology + Applications, 909804-909804, (2014).

[10] Chan, H. M., Parker, A. R., Piazza, A., and Richards, W. L., "Fiber-optic sensing system: Overview, development and deployment in flight at NASA," In Avionics and Vehicle Fiber-Optics and Photonics Conference (AVFOP), ThC2, 71-73, (2015).

[11] Ibrahim, S.K., O'Dowd, J., McCue, R., Honniball, A. and Farnan, M., "Design Challenges of a High Speed Tunable Laser Interrogator for Future Spacecraft Health Monitoring," CLEO: Applications and Technology, ATu1M-3, (2015).

[12] Mckenzie, I. and Karafolas, N., "Fiber optic sensing in space structures: the experience of the European Space Agency,"17th International Conference on Optical Fibre Sensors, Proc. SPIE 5855, 262-269, (2005).

[13] Schukar, V.G., Kusche, N. and Habel, W.R.,"How reliably do fiber Bragg grating patches perform as strain sensors?," IEEE Sensors Journal, 12(1), 128-132, (2012).

[14] Habel WR, Schukar V, and Hofmann D., "Requirements to Establish Fibre-Optic Sensors for Monitoring of Structures," EWSHM-7th European Workshop on Structural Health Monitoring, 2330-2337, (2014).

[15] Habel, WR., "Advances in Developing Standards for Fibre-Optic Sensors," 6th European Workshop on Structural Health Monitoring, Tu.4.C.3, (2012).

[16] Habel, W.R., Baumann, I., Berghmans, F., Borzycki, K., Chojetzki, C., Haase, K.H., Jaroszewicz, L.R., Kleckers, T., Niklès, M., Rothhardt, M. and Schlüter, V., "Guidelines for the characterization and use of fibre optic sensors: basic definitions and a proposed standard for FBG-based strain sensors," 20th International Conference on Optical Fibre Sensors, Proc SPIE 75035E, (2009).

[17] VDI-Standard: VDI/VDE 2660 Blatt 1, "Experimental stress analysis Optical strain sensor based on fibre Bragg grating," http://www.vdi.eu/guidelines/

[18] IEC 61757-1:2012, "Fibre optic sensors - Part 1: Generic specification", ISBN 978-2-83220-090-2, http://www.iec.ch/

[19] SEAFOM fiber optic monitoring group, http://www.seafom.com/

[20] IEEE (IC15-001-01), https://standards.ieee.org/about/sasb/iccom/IC15-001-01_Fiber_Optics_Sensors.pdf

[21] Gilbert, S.L., Swann, W.C. and Wang, C.M., "Hydrogen cyanide H13C14N absorption reference for 1530 nm to 1565 nm wavelength calibration–SRM 2519a," NIST special publication, 260, p.137, (2005).

[22] IEEE Ethernet standards, https://standards.ieee.org/findstds/standard/802.3-2008.html

[23] Kang, M.S., Yong, J.C. and Kim, B.Y., "Suppression of the polarization dependence of fiber Bragg grating interrogation based on a wavelength-swept fiber laser," Smart materials and structures, 15(2), 435, (2006).

[24] Berghmans, F., Geernaert, T., Baghdasaryan, T. and Thienpont, H., "Challenges in the fabrication of fibre Bragg gratings in silica and polymer microstructured optical fibres," Laser & Photonics Reviews, 8(1), 27-52, (2014).

[25] Chen, G., Liu, L., Jia, H., Yu, J., Xu, L., and Wang, W., "Simultaneous strain and temperature measurements with fiber Bragg grating written in novel Hi-Bi optical fiber," IEEE Photonics Technology Letters, 16(1), 221-223, (2004).
[26] Van Roosbroeck, J., Ibrahim, S.K., Lindner, E., Schuster, K. and Vlekken, J., "Stretching the Limits for the Decoupling of Strain and Temperature with FBG based sensors," International Conference on Optical Fibre Sensors (OFS24), 96343S-96343S, (2015).
[27] Sulejmani, S., Sonnenfeld, C., Geernaert, T., Mergo, P., Makara, M., Poturaj, K., Skorupski, K., Martynkien, T., Statkiewicz-Barabach, G., Olszewski, J. and Urbanczyk, W., "Control over the pressure sensitivity of Bragg grating-based sensors in highly birefringent microstructured optical fibers," IEEE Photonics Technology Letters, 24(6), 527-529, (2012).
[28] Liao, C.R. and Wang, D.N., "Review of femtosecond laser fabricated fiber Bragg gratings for high temperature sensing," Photonic Sensors, 3(2), 97-101, (2013).
[29] Canning, John, "Bragg Grating Sensors for Extreme Temperature Applications," In Frontiers in Optics 2014, FTu2B-1, (2014).
[30] Antonio-Lopez, J.E., Eznaveh, Z.S., LiKamWa, P., Schülzgen, A. and Amezcua-Correa, R., "Multicore fiber sensor for high-temperature applications up to 1000 C," Optics letters, 39(15), 4309-4312, (2014).
[31] Smit, M., Leijtens, X., Ambrosius, H., Bente, E., Van der Tol, J., Smalbrugge, B., De Vries, T., Geluk, E.J., Bolk, J., Van Veldhoven, R. and Augustin, L., "An introduction to InP-based generic integration technology. Semiconductor Science and Technology," 29(8), 083001, (2014).
[32] JePPIX roadmap 2015, http://www.jeppix.eu/document_store/JePPIXRoadmap2015.pdf
[33] EU project PARADAIGM, http://www.paradigm.jeppix.eu/